Permian pedoliths[25] and changed geomorphology as a result of rooted vegetation loss[26].

Regardless of the detailed mechanisms, the striking aspect of the Meishan 2-MHP profile is the presence of two distinct maxima within the investigated intervals. The pattern and cause of the marine mass extinction near the P/Tr boundary are still debated[8,12,27,28], in part because only faunal (and a small amount of calcareous algae) records of biotic change have been developed. A stepwise, multi-phase biotic extinction proposed by others on the basis of several southern China sections[12,27], has recently been challenged by a proposal of a main, sudden biotic crisis at beds 25–26 (ref. 28). However, the change in the 2-MHP index we report is equally dramatic (from minima to maxima) at both beds 25–26 and 28–29, such that a two-phase biotic crisis is supported not only by faunal extinctions, the interpretation of which has been the subject of debate, but also by substantial changes in the microbial community. The large changes in cyanobacterial population abundances revealed by the 2-MHP record, coupled with faunal mass extinction, probably indicate a stepwise and major environmental perturbation. Our study provides a window into the ecological restructuring, possibly at the base of the food chain, that occurred during this major faunal mass extinction. □

Methods

The solvents (HPLC grade) used were distilled twice. Tools used to prepare rock samples were rinsed with methanol and dichloromethane. Glassware was cleaned with detergent (Micro), rinsed with distilled water and annealed at 450 °C for 12 h. Aluminium foils were combusted at 450 °C for 12 h. Samples were processed in batches of six, including one procedural blank to monitor laboratory contamination.

The samples for lipid analysis were taken from section B and C at Meishan[9], 0.5–1.5 m back from the exposed cliff. The air-dried samples were ground to <80 mesh and 100–300 g Soxhlet-extracted with chloroform for 72 h with native copper added to remove sulphur. The extract was concentrated on a rotary evaporator under reduced pressure and transferred to a small vial. After evaporation of the remaining solvent, the total extractable lipid was weighed. The asphaltenes in the extracts were eliminated by precipitation in petroleum ether. The saturated hydrocarbons, aromatics and non-hydrocarbons were fractionated by column chromatography (silica gel 60), using sequential elution with petroleum ether, benzene and ethanol.

The saturated hydrocarbons were then analysed by GC/MS using a Hewlett-Packard 5973A MS, interfaced directly with a 6890 GC equipped with a HP-5MS fused silica capillary column (30 m × 0.25 mm inner diameter; 0.25 μm film thickness). The operating conditions were as follows: temperature ramped from 70 to 280 °C at 3 °C min^{-1} and held at 280 °C for 20 min with He as the carrier gas; the ionization energy of the mass spectrometer was set at 70 eV; the scan range was *m/z* 50–550. 2-MHP indices were calculated from the peak area of the compounds in mass chromatograms of *m/z* 191 (C_{30}) for αβ-hopane and *m/z* 205 (C_{31}) for its 2α-methyl analogue (similar profiles are generated if 2-MHP indices are calculated using higher molecular mass 2-MHPs and HPs). These are expressed as the 2-MHP index = (205/191) × 100. Sterane abundances used to calculate 2-MHP/sterane ratios were measured from the peak areas of the *m/z* 217 mass chromatograms. 2-MHPs were not detected in the procedural blanks using GC/MS analysis.

Received 26 August 2004; accepted 18 January 2005; doi:10.1038/nature03396.

1. Lehrmann, D. J. *et al.* Permian-Triassic boundary sections from shallow-marine carbonate platforms of the Nanpanjiang Basin, south China: Implications for oceanic conditions associated with the end-Permian extinction and its aftermath. *Palaios* **18,** 138–152 (2003).
2. Sheehan, P. M. & Harris, M. T. Microbialite resurgence after the Late Ordovician extinction. *Nature* **430,** 75–78 (2004).
3. Knoll, A. H. & Walter, M. W. Latest Proterozoic stratigraphy and Earth history. *Nature* **356,** 673–678 (1992).
4. Summons, R. E., Jahnke, L. L., Hope, J. M. & Logan, G. A. 2-Methylhopanoids as biomarkers for cyanobacterial oxygenic photosynthesis. *Nature* **400,** 554–557 (1999).
5. Simonin, P., Jurgens, U. J. & Rohmer, M. Bacterial triterpenoids of the hopane series from the prochlorophyte *Prochlorothrix hollandica* and their intracellular localization. *Eur. J. Biochem.* **241,** 865–871 (1996).
6. Rohmer, M., Bouvier-Nave, P. & Ourisson, G. Distribution of hopanoid triterpenes in prokaryotes. *J. Gen. Microbiol.* **130,** 1137–1150 (1984).
7. Rohmer, M., Bisseret, P. & Neunlist, S. in *Biological Markers in Sediments and Petroleum* (eds Moldowan, J. M., Albrecht, P. & Philp, R. P.) 1–17 (Prentice Hall, New Jersey, 1992).
8. Jin, Y. G. *et al.* Pattern of marine mass extinction near the Permian-Triassic boundary in South China. *Science* **289,** 432–436 (2000).
9. Yin, H., Zhang, K., Tong, J., Yang, Z. & Wu, S. The Global Stratotype Section and Point (GSSP) of the Permian-Triassic boundary. *Episodes* **24,** 102–114 (2001).
10. Brocks, J. J., Buick, R., Summons, R. E. & Logan, G. A. A reconstruction of Archean biological diversity based on molecular fossils from the 2.78 to 2.45 billion-year-old Mount Bruce Supergroup, Hamersley Basin, Western Australia. *Geochim. Cosmochim. Acta* **67,** 4321–4335 (2003).
11. Wignall, P. B. & Hallam, A. Griesbachian (Earliest Triassic) palaeoenvironmental changes in the Salt Range, Pakistan and Southeast China and their bearing on the Permian-Triassic mass extinction. *Palaeogeogr. Palaeoclimatol. Palaeoecol.* **102,** 215–237 (1993).
12. Yin, H. *et al. The Palaeozoic-Mesozoic Boundary, Candidates of Global Stratotype Section and Point of the Permian-Triassic Boundary* (China Univ. of Geosciences Press, Wuhan, 1996).
13. Lai, X., Wignall, P. & Zhang, K. Palaeoecology of the conodonts *Hindeodus* and *Clarkina* during the Permian-Triassic transitional period. *Palaeogeogr. Palaeoclimatol. Palaeoecol.* **171,** 63–72 (2001).
14. Yin, H. & Tong, J. Multidisciplinary high-resolution correlation of the Permian-Triassic boundary. *Palaeogeogr. Palaeoclimatol. Palaeoecol.* **143,** 199–212 (1998).
15. Hallam, A. & Wignall, P. *Mass Extinctions and their Aftermath* (Oxford Univ. Press, Oxford, 1997).
16. Valentine, J. W. & Jablonski, D. Mass extinctions: sensitivity of marine larval types. *Proc. Natl Acad. Sci. USA* **83,** 6912–6914 (1986).
17. Dionisio-Pires, L. M., Jonker, R. R., Van Donk, E. & Laanbroek, H. J. Selective grazing by adults and larvae of the zebra mussel (*Dreissena polymorpha*): application of flow cytometry to natural seston. *Freshwat. Biol.* **49,** 116–126 (2004).
18. Erwin, D. H. The end-Permian mass extinction. *Annu. Rev. Ecol. Syst.* **21,** 495–516 (1990).
19. Racki, G. Silica-secreting biota and mass extinctions: survival patterns and processes. *Palaeogeogr. Palaeoclimatol. Palaeoecol.* **154,** 107–132 (1999).
20. Keeling, M. J., Wilson, H. B. & Pacala, S. W. Reinterpreting space, time lags, and functional responses in ecological models. *Science* **290,** 1758–1761 (2000).
21. Erwin, D. H. Lessons from the past: biotic recoveries from mass extinction. *Proc. Natl Acad. Sci. USA* **98,** 5399–5403 (2001).
22. Vecoli, M. & Le Herisse, A. Biostratigraphy, taxonomic diversity and patterns of morphological evolution of Ordovician acritarchs (organic-walled microphytoplankton) from the northern Gondwana margin in relation to palaeoclimatic and palaeogeographic changes. *Earth-Sci. Rev.* **67,** 267–311 (2004).
23. Rampino, M. R. & Adler, A. C. Evidence for abrupt latest Permian mass extinction of foraminifera: results of tests for the Signor-Lipps effect. *Geology* **26,** 415–418 (1998).
24. Mastin, B. J., Rodger, J. H. Jr & Deardorff, T. L. Risk evaluation of cyanobacteria-dominated algal blooms in a North Louisiana reservoir. *J. Aquatic Ecosyst. Stress Recovery* **9,** 103–114 (2002).
25. Retallack, G. J. Search for evidence of impact at the Permian-Triassic boundary in Antarctica and Australia. *Geology* **26,** 979–982 (1998).
26. Ward, P. D., Montgomery, D. R. & Smith, R. Altered river morphology in South Africa related to the Permian-Triassic extinction. *Science* **289,** 1740–1743 (2000).
27. Yang, Z. Y. *et al. Permo-Triassic Events of South China* (Geological Publishing House, Beijing, 1993).
28. Erwin, D. H., Bowring, S. A. & Jin, Y. in *Special Paper 356, Catastrophic Events and Mass Extinctions: Impacts and Beyond* (eds Koeberl, C. & MacLeod, K. G.) 363–383 (Geological Society of America, Boulder, 2002).

Supplementary Information accompanies the paper on **www.nature.com/nature**.

Acknowledgements We thank F. Yang, S. Wu, G. Zhu, J. Huang, Y. Yi and J. Yu for field assistance, L. Lu, D. Jiao and X. Huang for sample processing, and M. Benton for constructive comments on the manuscript. The authors thank I. D. Bull and R. Berstan for their technical assistance and the NERC for funding the Bristol node of the Life Sciences Mass Spectrometry Facility (http://www.chm.bris.ac.uk/lsmsf/index.html). This work was supported by National Natural Science Foundation (H. Y.), NCET programme of Ministry of Education of China (S. X.) and the Lab of Bio- and Environmental Geology in China University of Geosciences.

Competing interests statement The authors declare that they have no competing financial interests.

Correspondence and requests for materials should be addressed to R.D.P. (r.d.pancost@bristol.ac.uk).

Affinities of 'hyopsodontids' to elephant shrews and a Holarctic origin of Afrotheria

Shawn P. Zack[1], Tonya A. Penkrot[1], Jonathan I. Bloch[2] & Kenneth D. Rose[1]

[1]*Center for Functional Anatomy and Evolution, The Johns Hopkins University School of Medicine, 1830 East Monument Street, Baltimore, Maryland 21205, USA*
[2]*Florida Museum of Natural History, University of Florida, Gainesville, Florida 32611-7800, USA*

Macroscelideans (elephant shrews or sengis) are small-bodied (25–540 g), cursorial (running) and saltatorial (jumping), insectivorous and omnivorous[1] placental mammals represented by at least 15 extant African species classified in four genera[2]. Macroscelidea is one of several morphologically diverse but predominantly African placental orders classified in the superorder

Afrotheria by molecular phylogeneticists[3,4]. The distribution of modern afrotheres, in combination with a basal position for Afrotheria within Placentalia and molecular divergence-time estimates, has been used to link placental diversification with the mid-Cretaceous separation of South America and Africa[4]. Morphological phylogenetic analyses do not support Afrotheria[5–7] and the fossil record favours a northern origin of Placentalia[8]. Here we describe fossil postcrania that provide evidence for a close relationship between North American Palaeocene–Eocene apheliscine 'hyopsodontid' 'condylarths' (early ungulates or hoofed mammals) and extant Macroscelidea. Apheliscine postcranial morphology is consistent with a relationship to other ungulate-like afrotheres (Hyracoidea, Proboscidea) but does not provide support for a monophyletic Afrotheria. As the oldest record of an afrothere clade, identification of macroscelidean relatives in the North American Palaeocene argues against an African origin for Afrotheria, weakening support for linking placental diversification to the break-up of Gondwana.

Molecular analyses that place Macroscelidea within Afrotheria also include tenrecid and chrysochlorid insectivores, paenungulates (hyracoids, proboscideans and sirenians), and tubulidentates[3,4] in this clade, a diverse assemblage of predominantly African placentals. Morphologists have proposed a relationship for Macroscelidea to either Glires (rodents and rabbits)[9–11] or to Ungulata[12–15], the latter also supported by behavioural observations[2]. Morphologists

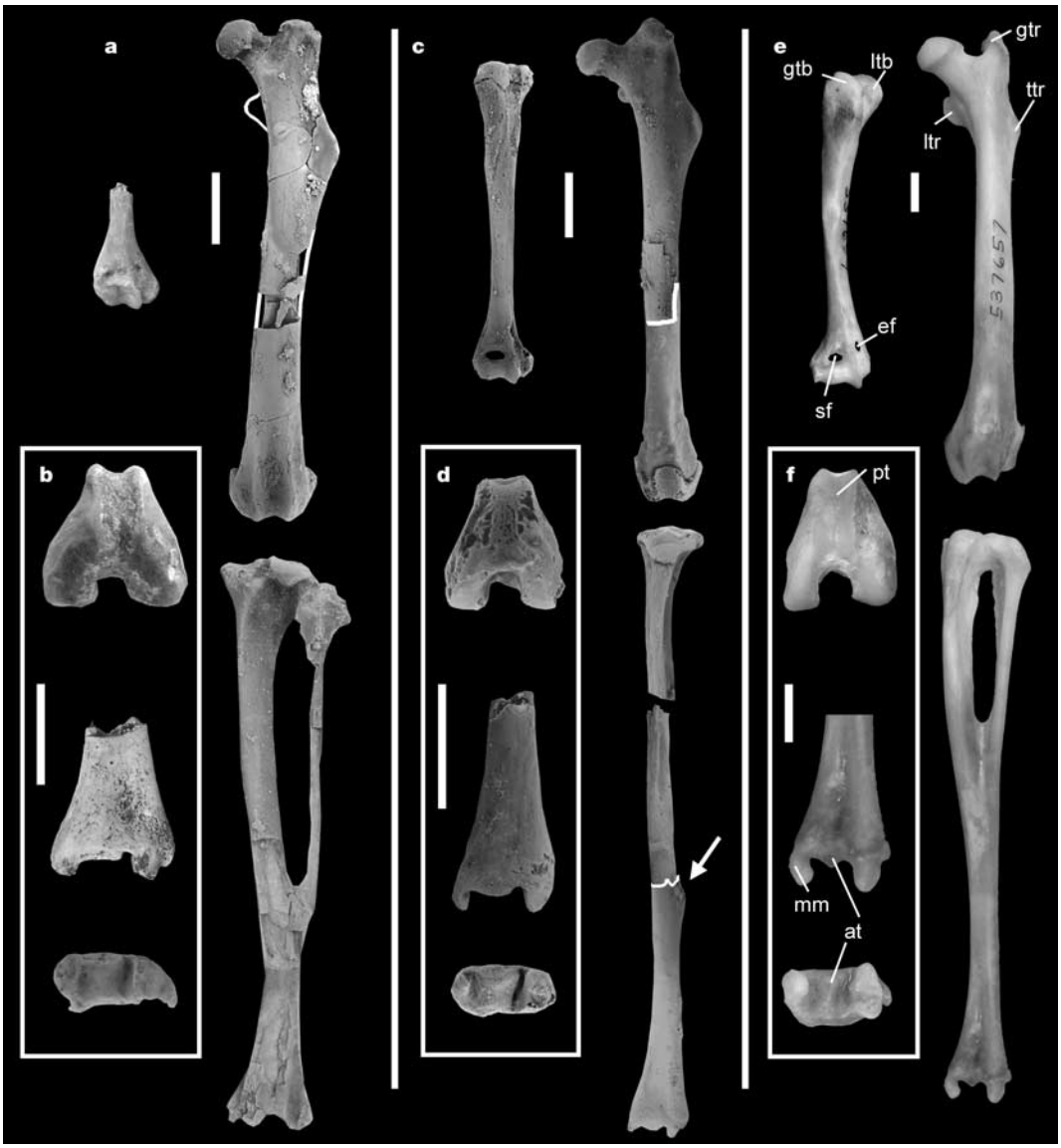

Figure 1 Comparison of apheliscine and macroscelidean long bones. Long bones of *Apheliscus* (**a**, **b**), *Haplomylus* (**c**, **d**), and the macroscelidean *Rhynchocyon* (**e**, **f**). Elements in **a**, **c** and **e** (clockwise from top left): right humerus, left femur and left fused tibia and fibula in anterior view except *Apheliscus* tibia-fibula (in posterior view). Elements in **b**, **d** and **f** (top to bottom): left distal femur in distal view, distal tibia-fibula in anterior view, and distal tibia-fibula in distal view. Some elements are reversed for clarity. Scale bars, 5 mm. Arrow in **c** indicates the most proximal point of fusion of the tibia and fibula. at, anterior tubercle; ef, entepicondylar foramen; gtb, greater tuberosity; gtr, greater trochanter; ltb, lesser tuberosity; ltr, lesser trochanter; mm, medial malleolus; pt, patellar groove; sf, supratrochlear foramen; ttr, third trochanter. Specimens illustrated (United States National Museum (USNM); Department of Paleobiology (**a**–**d**) and Department of Mammalogy (**e**–**f**)): **a**, 493903 (humerus), 488326 (femur, ltr reconstructed from 525593), 495051 (tibia-fibula); **b**, 493819 (femur), 493903 (tibia-fibula); **c**, 513512 (humerus), 513057 (proximal femur), 513140 (distal femoral shaft), 513173 (distal femoral epiphysis), 513245 (proximal tibia), 513868 (tibia-fibula); **d**, 513173 (femur), 513239 (tibia-fibula); **e**–**f**, 537657. See Supplementary Information for a full list of specimens examined.

include artiodactyls, perissodactyls, paenungulates, possibly tubulidentates, and extinct groups, particularly the paraphyletic basal order 'Condylarthra'[9,16,17], in Ungulata. The fossil record of macroscelideans extends to the African late early Eocene[12], and these dental fossils suggest affinities to the polyphyletic[15,18] 'condylarth' family 'Hyopsodontidae'. However, *Hyopsodus*, the only skeletally well-known 'hyopsodontid', differs markedly from macroscelideans[19].

A new dentally associated skeleton of *Apheliscus chydaeus* (USNM 525597) includes portions of all long bones and several foot bones, allowing identification of other isolated bones from Willwood Formation quarries (early Eocene, Bighorn Basin, Wyoming). Direct associations of dental and postcranial material remain unknown for *Haplomylus*, but a convincing case for the reassociation of isolated postcranial elements can be made on the basis of size, relative abundance, stratigraphic distribution and especially morphologic similarity to those of *Apheliscus*. Dental morphology has been used to link *Apheliscus* and *Haplomylus* (referred to informally as apheliscines), along with other 'Hyopsodontidae'[20,21].

Apheliscine postcrania indicate a similar body mass to the extant forest elephant shrew *Petrodromus tetradactylus* (160–280 g[22]) and specializations for rapid terrestrial locomotion, as in extant cursorial and saltatorial mammals (see Supplementary Information for modern taxa examined). The combination of specializations in apheliscines is uniquely similar to living and extinct macroscelideans, suggesting a close phylogenetic relationship.

In the forelimb, the distal humerus has a weak supinator crest and a reduced medial epicondyle. The olecranon fossa is deep (*Apheliscus*) or perforate (*Haplomylus*), indicating capacity for full extension at the elbow. The capitulum is ovoid and the trochlea has a sharply distally projecting medial rim, whereas the ovoid proximal radius has a flat ulnar articulation, indicating little or no ability to supinate the forearm (Fig. 1a, c).

Features of the femur indicate specialization for rapid terrestrial locomotion. Proximally, the greater trochanter is even with (*Apheliscus*) or slightly higher (*Haplomylus*) than the small femoral head. The femoral neck is short and distinct. The lesser trochanter is directed posteromedially, whereas the third trochanter is strong and proximally positioned. Distally, the femur is anteroposteriorly deep, with anteriorly extensive condylar articular surfaces, permitting full knee extension, whereas the patellar groove is narrow, deep, elevated and proximally extensive.

Specializations for cursoriality are also found in the crus. The proximal tibia has a sharp cnemial crest that extends only one-quarter (*Haplomylus*) to one-third (*Apheliscus*) the length of the bone, indicating capability for rapid extension at the knee. The gracile shafts of the tibia and fibula are completely synostosed over the distal one-third (*Apheliscus*) to one-half (*Haplomylus*) of their

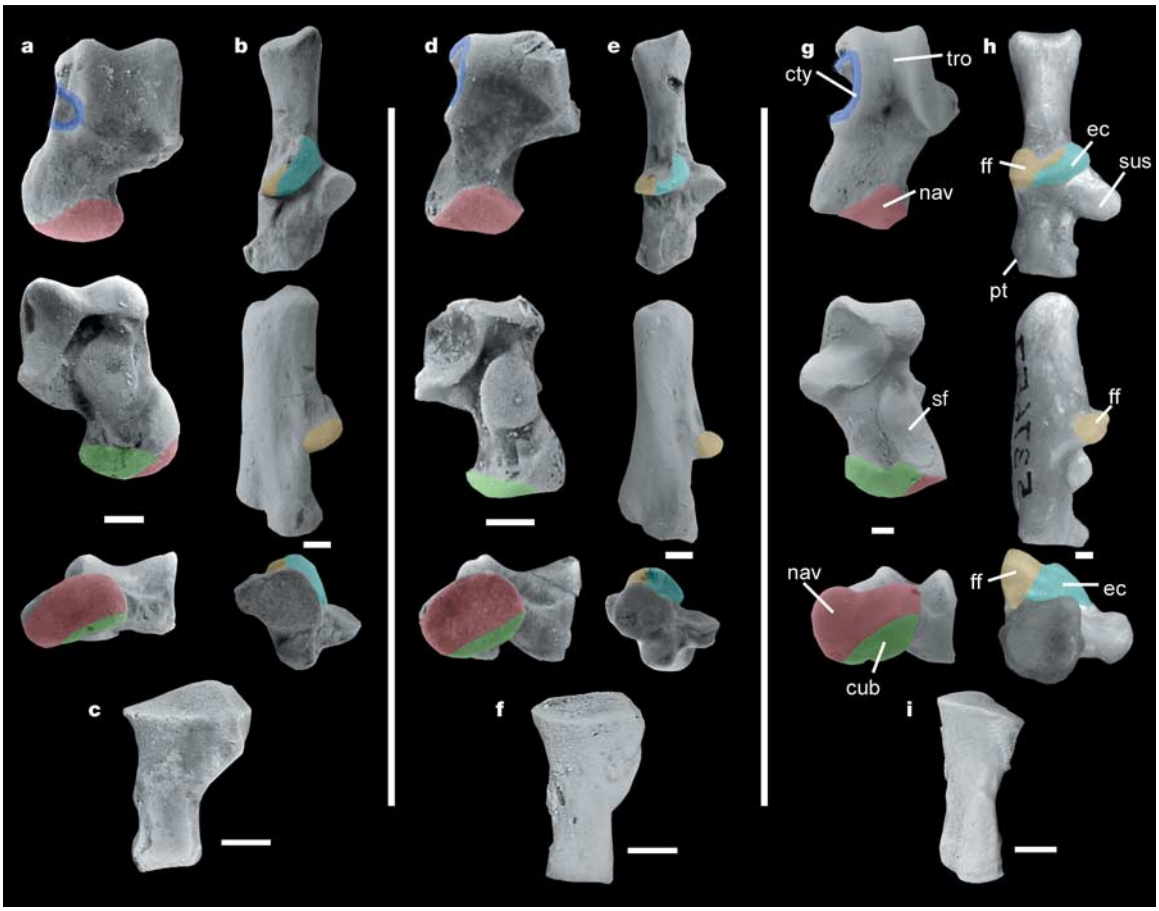

Figure 2 Comparison of apheliscine and macroscelidean tarsals. Left astragali (**a**, **d**, **g**), right calcanei (**b**, **e**, **h**) and cuboids (**c**, **f**, **i**) of *Apheliscus* (**a**–**c**), *Haplomylus* (**d**–**f**), *Rhynchocyon* (**g**, **h**) and *Petrodromus* (**i**). Astragali illustrated in dorsal (top), ventral (middle) and distal (bottom) views. Calcanei illustrated in dorsal (top), lateral (middle) and distal (bottom) views. Cuboids illustrated in dorsal view. Some elements are reversed for clarity. Scale bars, 1 mm. cty, cotylar fossa (dark blue); cub, cuboid facet (green); ec, ectal facet (light blue); ff, fibular facet (yellow); nav, navicular facet (red); pt, peroneal tubercle; sf, sustentacular facet (astragalar); sus, sustentacular facet (calcaneal); tro, trochlea. Specimens illustrated (USNM; Department of Paleobiology (**a**–**f**) and Department of Mammalogy (**g**–**i**)): **a**, 521791; **b**, 521789; **c**, 513632; **d**, 493901; **e**–**f**, 537657.

length. The tibia is longer than the femur, an estimation based on unassociated elements (Fig. 1).

In the tarsus, the astragalar trochlea is deeply grooved and lacks an astragalar foramen. The astragalar neck is elongate. The axis of curvature of the navicular facet on the astragalar head indicates predominance of parasagittal movements at the transverse tarsal joint. Characteristic of digitigrade mammals (in which weight is supported on distal phalangeal segments) such as modern dogs, cats and rabbits, the calcaneal tuber is elongate and gracile. The body of the calcaneum is elongate, and the peroneal tubercle is small (*Apheliscus*) or almost absent (*Haplomylus*), and is situated at the distal margin of the calcaneum (Fig. 2). On the cuboid, the metatarsal facet is flat and faces distally (not distolaterally), suggesting a columnar metatarsus (again implying digitigrady).

The characteristics described above are present in diverse extant cursorial and saltatorial mammals, but the combination in apheliscines occurs only in macroscelideans. Additional postcranial features infrequently encountered among mammals further support a special relationship between apheliscines and macroscelideans. In *Apheliscus*, the proximal fibula is enlarged and contributes to the posterolateral corner of the knee joint, a trait elaborated on in macroscelideans. The proximal fibula is unknown in *Haplomylus*, but facets on the tibia indicate further expansion onto the lateral margin of the lateral tibial condyle. In apheliscines, the medial malleolus of the distal tibia is enlarged to form a laterally recurved hook-like process, whereas the central portion of the deeply grooved distal tibial articular surface slopes anteroventrally to form a distinctive anterior tubercle. Both of these features are shared with macroscelideans, as is the presence of a well-developed cotylar fossa—larger in *Haplomylus* than in *Apheliscus*—that articulates with the tibial malleolus on the medial aspect of the astragalar body. A large cuboid facet is present on the astragali of both apheliscines, and the boundary between the cuboid and navicular facets is sharp in *Haplomylus*, another similarity to macroscelideans. In *Haplomylus*, as in macroscelideans, the angle between the proximal and distal portions of the calcaneal ectal facet is sharp, restricting mobility between the astragalus and calcaneum. Apheliscines resemble macroscelideans in having a large calcaneal fibular facet whose axis of curvature parallels that of the astragalar trochlea (Fig. 2). Finally, apheliscines share an elongate cuboid with macroscelideans (Fig. 2c,f,i). The combination of these distinctive features is found only in apheliscines and macroscelideans, providing particularly powerful evidence for a close relationship, although no individual feature is unique. This is strengthened by previous phylogenetic hypotheses, based on dental anatomy, that some 'hyopsodontids'—particularly *Haplomylus*—and macroscelideans are closely related[13,14].

In view of proposed relationships of Macroscelidea to Glires (in the superorder Anagalida), Ungulata (as traditionally defined to include paenungulates), or Afrotheria, we tested the hypothesized macroscelidean affinities of *Apheliscus* and *Haplomylus* using three character-taxon matrices: two previously published that extensively sample Anagalida and Afrotheria, respectively[7,11], and a new matrix that samples basal members of Ungulata (Supplementary Information). Phylogenetic analyses of all three matrices, using the parsimony ratchet algorithm of NONAv2.0 implemented using Winclada(BETA)v0.9.9, place apheliscines on the macroscelidean stem, with *Haplomylus* as the sister taxon to extant African macroscelideans (Fig. 3). Results from our new analysis indicate that the European louisinine 'hyopsodontid' *Paschatherium* (known from dentitions and tarsal bones) is the sister taxon to the clade that includes apheliscines and extant African Macroscelidea. *Hyopsodus* is not closely related to extant Macroscelidea or apheliscines in any of the three analyses, supporting a polyphyletic 'Hyopsodontidae'.

Identification of a relationship between apheliscines and macroscelideans has direct significance to a discussion of the higher-level affinities of Macroscelidea. A close relationship between Glires and macroscelideans is not supported by dental (apheliscines and early macroscelideans are more ungulate-like[12–15]) or postcranial morphology (apheliscines lack anagalidan characteristics such as a posterior process on the distal tibia). Because most character evidence recently cited in support of Anagalida is cranial[9,10], we cannot definitively reject anagalidan affinities for Macroscelidea, but the known morphology of *Apheliscus* and *Haplomylus* argues against such a relationship.

On the basis of dental morphology[16–18,21] most authors have placed *Haplomylus* and *Apheliscus* in the basal ungulate order 'Condylarthra', and it is not surprising that apheliscine dentitions are more congruent with ungulate affinities for Macroscelidea. The general postcranial resemblance of apheliscines to many ungulates, particularly artiodactyls, perissodactyls and phenacodontid 'condylarths', probably reflects similar adaptations for rapid terrestrial locomotion[23]. The lack of more distinctive derived features in common with any of those groups (for example, the double-pulley

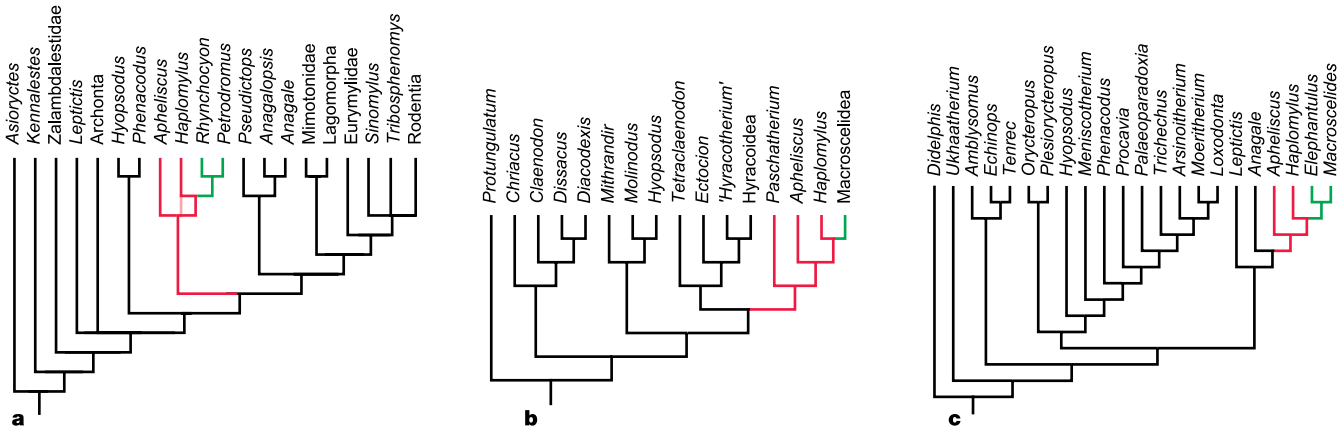

Figure 3 Phylogenetic relationships of apheliscines. **a**, Strict consensus of 16 most parsimonious trees from reanalysis of the ref. 11 character-taxon matrix with some characters ordered (length, L: 979; consistency index, CI: 39; retention index, RI: 77). For visual simplicity, some clades are collapsed into single terminal taxa. Faint red line: position of *Haplomylus* in strict consensus of twelve most parsimonious trees with all characters unordered (L: 926; CI: 41; RI: 76). **b**, Single most parsimonious tree from analysis of basal ungulates with all characters unordered (L: 180; CI: 38; RI: 47) or with some characters ordered (L: 181; CI: 38; RI: 48). **c**, Single most parsimonious tree derived from reanalysis of the ref. 7 character-taxon matrix with all characters unordered and only afrotheres and their potential extinct relatives included (L: 380; CI: 45; RI: 58). In all trees, macroscelideans are indicated in green, whereas red indicates apheliscines (and *Paschatherium* in **b**).

astragalus of artiodactyls) indicates that these similarities represent homoplasies rather than synapomorphies.

The cotylar fossa (and associated enlarged medial malleolus), present in apheliscines and macroscelideans, is shared with hyracoids, proboscideans, tubulidentates, and their possible extinct relatives *Meniscotherium* and *Plesiorycteropus*[24–26]. Living members of this assemblage of mammals have been classified in Ungulata by morphological systematists, but in Afrotheria by molecular systematists. Presence of a cotylar fossa does not seem to be associated with any particular mode of locomotion, because it occurs in fossorial (Tubulidentata, *Plesiorycteropus*) and scansorial (Hyracoidea) mammals, as well as in the cursorial/saltatorial macroscelideans. The cotylar fossa is also present in cercopithecoid primates and macropodid marsupials[25,27], and is therefore not unique to potential afrotheres, but it is absent in most mammals, including other cursorial and saltatorial mammals. The broad functional but restricted taxonomic distribution of the cotylar fossa makes it a potentially significant indicator of phylogenetic affinities and argues for a relationship of apheliscines and macroscelideans to hyracoids, proboscideans and tubulidentates. The combination of dental and tarsal characters in apheliscines is most consistent with a relationship to Hyracoidea and Proboscidea, regardless of whether these taxa are classified in Afrotheria or a monophyletic Ungulata.

Identification of North American sister taxa to Macroscelidea suggests a North American origin for the order and a non-African origin for Afrotheria. Present evidence indicates that the restriction of Macroscelidea to Africa from the middle Eocene to the present is either relictual or (more likely) indicative of Palaeocene or Eocene dispersal to Africa. Therefore, the subsequent distribution of Macroscelidea no longer supports an African origin. Because Holarctic Palaeocene apheliscines and *Paschatherium* potentially represent the oldest known afrotheres, a non-African origin or relictual distribution is also implied for Afrotheria, a supposition supported by early non-African records of sirenians[28], proboscideans[29] and possibly tubulidentates[30]. Neither possibility supports claims that Placentalia originated in Gondwana, which are based partly on the assumption of an African origin for Afrotheria[4]. This conclusion agrees with that of a recent phylogenetic analysis combining morphologic and molecular data that suggested paenungulate affinities for other North American 'condylarths'[7]. □

Received 22 June 2004; accepted 11 January 2005; doi:10.1038/nature03351.

1. Kingdon, J. *East African Mammals. Volume IIA: Insectivores and Bats* (Univ. Chicago Press, Chicago, 1974).
2. Rathbun, G. B. The social structure and ecology of elephant-shrews. *Z. Tierpsychol.* **20** (suppl.), 1–77 (1979).
3. Stanhope, M. J. *et al.* Molecular evidence for multiple origins of Insectivora and for a new order of endemic African insectivore mammals. *Proc. Natl Acad. Sci. USA* **95,** 9967–9972 (1998).
4. Murphy, W. J. *et al.* Resolution of the early placental mammal radiation using Bayesian phylogenetics. *Science* **294,** 2348–2351 (2001).
5. Asher, R. J. A morphological basis for assessing the phylogeny of the "Tenrecoidea" (Mammalia, Lipotyphla). *Cladistics* **15,** 231–252 (1999).
6. Whidden, H. P. Extrinsic snout musculature in Afrotheria and Lipotyphla. *J. Mammal. Evol.* **9,** 161–184 (2002).
7. Asher, R. J., Novacek, M. J. & Geisler, J. H. Relationships of endemic African mammals and their fossil relatives based on morphological and molecular evidence. *J. Mammal. Evol.* **10,** 131–194 (2003).
8. Archibald, J. D. Timing and biogeography of the eutherian radiation: fossils and molecules compared. *Mol. Phylogenet. Evol.* **28,** 350–359 (2003).
9. Novacek, M. J. The skull of leptictid insectivorans and the higher-level classification of eutherian mammals. *Bull. Am. Mus. Nat. Hist.* **183,** 1–111 (1986).
10. Novacek, M. J. & Wyss, A. Higher-level relationships of the recent eutherian orders: morphological evidence. *Cladistics* **2,** 257–287 (1986).
11. Meng, J., Hu, Y. & Li, C. The osteology of *Rhombomylus* (Mammalia, Glires): implications for phylogeny and evolution of Glires. *Bull. Am. Mus. Nat. Hist.* **275,** 1–247 (2003).
12. Hartenberger, J.-L. Hypothèse paléontologique sur l'origine des Macroscelidea (Mammalia). *C.R. Acad. Sci. II* **302,** 247–249 (1986).
13. Simons, E. L., Holroyd, P. A. & Bown, T. M. Early Tertiary elephant-shrews from Egypt and the origin of the Macroscelidea. *Proc. Natl Acad. Sci. USA* **88,** 9734–9737 (1991).
14. Butler, P. M. Fossil Macroscelidea. *Mamm. Rev.* **25,** 3–14 (1995).
15. Tabuce, R., Coiffait, B., Coiffait, P.-E., Mahboubi, M. & Jaeger, J.-J. A new genus of Macroscelidea (Mammalia) from the Eocene of Algeria: a possible origin for elephant-shrews. *J. Vertebr. Paleontol.* **21,** 535–546 (2001).
16. McKenna, M. C. & Bell, S. K. *Classification of Mammals Above the Species Level* (Colombia Univ. Press, New York, 1997).
17. Archibald, J. D. in *Evolution of Tertiary Mammals of North America. Volume 1: Terrestrial Carnivores, Ungulates, and Ungulatelike Mammals* (eds Janis, C. M., Scott, K. M. & Jacobs, L. L.) 292–331 (Cambridge Univ. Press, Cambridge, 1998).
18. Cifelli, R. L. The origin and affinities of the South American Condylarthra and early Tertiary Litopterna (Mammalia). *Am. Mus. Novit.* **2772,** 1–48 (1983).
19. Gazin, C. L. A study of the Eocene condylarthran mammal *Hyopsodus*. *Smithson. Misc. Coll.* **153,** 1–90 (1968).
20. Van Valen, L. M. New Paleocene insectivores and insectivore classification. *Bull. Am. Mus. Nat. Hist.* **135,** 217–284 (1967).
21. Rose, K. D. The Clarkforkian land-mammal age and mammalian faunal composition across the Paleocene-Eocene boundary. *Univ. Mich. Pap. Paleontol.* **26,** 1–197 (1981).
22. Jennings, M. R. & Rathbun, G. B. Petrodromus tetradactylus. *Mamm. Species* **682,** 1–6 (2001).
23. Rose, K. D. Postcranial skeletal remains and adaptations in early Eocene mammals from the Willwood Formation, Bighorn Basin, Wyoming. *Spec. Pap. Geol. Soc. Am.* **243,** 107–133 (1990).
24. Court, N. Limb posture and gait in *Numidotherium koholense*, a primitive proboscidean from the Eocene of Algeria. *Zool. J. Linn. Soc.* **111,** 297–338 (1994).
25. MacPhee, R. D. E. Morphology, adaptations, and relationships of *Plesiorycteropus*, and a diagnosis of a new order of eutherian mammals. *Bull. Am. Mus. Nat. Hist.* **220,** 1–214 (1994).
26. Godinot, M., Smith, T. & Smith, R. Mode de vie et affinités de *Paschatherium* (Condylarthra, Hyopsodontidae) d'après ses os du tarse. *Palaeovertebrata* **25,** 225–242, plate 1–2 (1996).
27. Szalay, F. S. *Evolutionary History of the Marsupials and an Analysis of Osteological Characters* (Cambridge Univ. Press, Cambridge, 1994).
28. Savage, R. J. G., Domning, D. P. & Thewissen, J. G. M. Fossil Sirenia of the West Atlantic and Caribbean region. V. The most primitive known sirenian, *Prorastomus sirenoides* Owen, 1855. *J. Vertebr. Paleontol.* **14,** 427–449 (1994).
29. Ginsburg, L., Durrani, K. H., Kassi, A. M. & Welcomme, J.-L. Discovery of a new Anthracobunidae (Tethytheria, Mammalia) from the lower Eocene lignite of the Kach-Harnai area in Baluchistan (Pakistan). *C.R. Acad. Sci. IIa* **328,** 209–213 (1999).
30. Thewissen, J. G. M. Cephalic evidence for the affinities of Tubulidentata. *Mammalia* **49,** 257–284 (1985).

Supplementary Information accompanies the paper on **www.nature.com/nature**.

Acknowledgements We would like to thank: T. M. Bown, for collection of the original *Apheliscus* skeletal association; D. Diveley, J. Meng (American Museum of Natural History), R. Emry, L. Gordon, H. Kafka, J. Mead, R. Purdy (USNM) and P. Houde (New Mexico State University) for access to specimens; D. M. Boyer for helpful discussions; J. C. Mussell for advice and comments on the manuscript; and D. B. Weishampel for access to equipment and facilities. We would also like to thank G. B. Rathbun for access to high quality images of sengis. Support of fieldwork leading to these discoveries has been provided by the US National Science Foundation and the Bureau of Land Management.

Competing interests statement The authors declare that they have no competing financial interests.

Correspondence and requests for materials should be addressed to S.P.Z. (szack1@jhem.jhmi.edu).

Evidence that sensory traps can evolve into honest signals

Constantino Macías Garcia & Elvia Ramirez

Departamento de Ecología Evolutiva, Instituto de Ecología, UNAM, AP 70-275, CP 04510 México DF, México

Conventional models[1–4] explaining extreme sexual ornaments propose that these reflect male genetic quality[2–4] or are arbitrary results of genetic linkage between female preference and the ornament[1]. The chase-away model[5] emphasizes sexual conflict: male signals attract females because they exploit receiver biases[6–9]. As males gain control of mating decisions, females may experience fitness costs through suboptimal mating rates or post-copulatory exploitation. Elaboration of male signals is expected if females increase their response threshold to resist such exploitation. If ornaments target otherwise adaptive biases such as feeding responses[8–10], selection on females might eventually separate sexual and non-sexual responses to the signal. Here we show that the terminal yellow band (TYB) of several Goodeinae species evokes both feeding and sexual responses; sexual